Content list available at BioEnv

Bioresources and Environment

Journal homepage: www.bioenvuitm.com

Nanocellulose from Banana Pseudostem for Pb^{2+} and Cd^{2+} Ions Removal from Aqueous Solutions

Bassim Mohammed Al-Dabash,[1*] Mohamed Saleh Al-Kahali [2]

[1]*Department of Chemistry, Sabr Faculty of Science and Education, Lahj University, Yemen*

[2]*Department of Chemistry, Faculty of Science, Aden University, Yemen*

Received December 27, 2024, Accepted in revised form February 21, 2025
Available online February 27, 2025

ABSTRACT. The aim of this study was to investigate the removal of Pb and Cd ions from aqueous solutions using Nanocellulose (NC) extracted from banana pseudostem fiber. The microstructure and properties of nanocellulose were characterized using various techniques, including Fourier transform infrared (FTIR), transmission electron microscopy (TEM), energy dispersive X-ray (EDX) coupled with field emission scanning electron microscopy (FE-SEM), and Brunauer-Emmett-Teller (BET) analysis. The adsorption process was evaluated by analyzing several influencing factors, including pH (3 –7), contact time (20 – 100 min), initial concentration (10 – 50 mg/L), and adsorbent dose (0.05 – 0.25 g). The kinetics of adsorption were studied using the pseudo-first-order and pseudo-second-order models, while the adsorption isotherms were analyzed using the Langmuir and Freundlich models. Optimal adsorption conditions were determined to be pH 5 for Pb^{2+} and pH 6 for $Cd^{2+,}$ with a contact time of 60 minutes. The NC achieved adsorption percentages of 96.22% and 92.5% for Pb^{2+} and Cd^{2+}, respectively, with corresponding adsorption capacities of 24.02 mg/g and 20.54 mg/g. The findings demonstrate that the adsorption process of Pb^{2+} and Cd^{2+} onto the surface of NC followed the 2nd order kinetic, as evidenced by the high values of (R^2) 0.98019 and 0.98428 for Pb and Cd ions, respectively, compared to the 1st order model with values of 0.8048 and 0.67804. Furthermore, the Langmuir model was found to be a better fit for the adsorption process, with (R^2) values of 0.97001 and 0.94761 for lead and cadmium ions, respectively, compared to the Freundlich model with values of 0.93307 and 0.9086. The BET analysis showed a surface area of 52.3891 m^2/g for NC. The results of the adsorption process at optimal conditions indicate that the surface of the NC is somewhat effective in the adsorption of lead and cadmium ions from aqueous solutions. This indicates its potential for application in water treatment, especially for industrial wastewater remediation.

Key words: Nanocellulose, Adsorption, Heavy Metal Pollutants, Nanotechnology.

1. INTRODUCTION

In recent years, there has been a notable rise in domestic chores, agricultural activities, and industrial operations globally, resulting in the discharge of numerous contaminants into aquatic ecosystems (Aziz et al., 2023). These contaminants comprise hazardous heavy metals, which provide a significant risk to both human health and the ecology (Mitra et al., 2022). Heavy metal contamination has emerged as a significant issue owing to its toxicity and detrimental effects on living creatures (Mitra et al., 2022; Briffa et al., 2020). Heavy metals can interfere with the body's metabolic functions, even at minimal amounts. The ingestion of drinking water polluted with lead (Pb) can result in neonatal fatalities, infertility, gastrointestinal discomfort, and harm to the liver, kidneys, and brain (Tchounwou et al., 2012). Likewise, exposure to cadmium can result in grave repercussions, including cancer, hypertension, peripheral nervous system damage, and impairment of lung and kidney function. It is imperative that we confront these concerns and implement appropriate actions to alleviate the effects of heavy metal pollution on our

*Corresponding author: Tel.: +967773746685
E-mail address: *basmalrbash26@gmail.com* (Bassim Mohammed Al-Dabash)

environment and health (Rafati Rahimzadeh et al., 2017).

A variety of techniques have been employed to eliminate heavy metals from contaminated water sources. The procedures comprise sedimentation, chemical reduction, adsorption, ion exchange, lime precipitation, membrane filtering, and solvent extraction (Yadav et al. 2021; Isawi, 2020). Each of these systems possesses distinct advantages and downsides, including elevated costs, significant time investment, and substantial material expenses. These processes are expensive and labor-intensive, with the exception of adsorption. Adsorption is the predominant method employed for water treatment, attributed to its advantageous characteristics, including operational simplicity, energy efficiency, liquid sludge generation, and rapid pollutant recovery (Ariffin et al., 2017; Akhtar et al., 2025). Adsorption entails physical and chemical interactions between metal ions and diverse functional groups, such as sulfate, phosphate, amino, and carboxyl (Mahfoudhi & Boufi, 2017; Kaur et al., 2020; Kara et al., 2021).

Recent advancements in nanotechnology have suggested the application of nanomaterials for the remediation of water contamination caused by heavy metals, owing to their beneficial qualities (Ahmad & Mirza, 2018). Plant extracts are crucial in the development of sustainable nano biomaterials because of their abundant availability as renewable resources. Among these extracts, cellulose is the most abundant, providing solutions to issues with material renewal, toxicity, cost, energy consumption, and biodegradability (Reshmy et al., 2022; Wang et al., 2019). This carbohydrate, derived from biomass such as agricultural by-products, forest leftovers, and diverse plant materials, signifies a viable method for generating value-added products (Blasi et al., 2023).

Nanocellulose derived from cellulose sourced from biomass waste has garnered considerable scientific interest owing to its biodegradability, regenerative capabilities, distinctive chemical and physical properties, as well as its extensive applications (Tshikovhi et al., 2020; Panchal et al., 2018). It is a biopolymer that can exist in the form of fibers or crystals with nanometer dimensions and a diameter of less than 100 nm (Mo et al., 2020). Cellulose possesses a surface abundant in reactive hydroxyl groups, facilitating the alteration of nanocellulose and enhancing its efficacy (Tshikovhi et al., 2020; Kim et al., 2016; Grishkewich et al., 2017).

The banana pseudostem fiber, characterized by its abundance, elevated cellulose content, cost-effectiveness, and renewability relative to other biomass, has been thoroughly investigated as an adsorbent for water treatment, encompassing the extraction of metal ions, dyes, pesticides, inorganic cations, and various organic compounds in water and wastewater (Ali, 2017; Farias et al., 2023). A viable approach to augment the value of banana biomass is through the extraction of Nanocellulose (NC) from this material. Banana waste is rich in lignocellulosic components, including hemicellulose, cellulose, and lignin, rendering it a significant source for nanocellulose extraction (Zaini et al., 2023). The abundance of functional groups, including thiol, amino, and ester groups, on the surface of extracted NC renders it a promising, cost-effective renewable adsorbent for the removal of pollutants from water (Ram & Chauhan, 2018).

This study involved the processing of readily accessible banana pseudostem fiber in a local setting, where cellulose

was extracted and transformed into nanocellulose using acid hydrolysis and mechanical agitation with ultrasonication. The characterisation was conducted to investigate the microstructure and properties of nanocellulose, employing FT-IR to assess chemical structure, while the dimensions of the nanocellulose were ascertained using TEM. Elemental surface analysis was conducted via EDX, whereas surface area and pore diameter were evaluated using BET. Nanocellulose was employed to eliminate lead (Pb) and cadmium (Cd) ions from aqueous solutions, considering several parameters that influence the adsorption process. The parameters encompass pH, contact duration, starting ion concentration, and the quantity of adsorbent utilized. The research examined the kinetics and adsorption isotherms of Pb^{2+} and Cd^{2+} ions on the surface of nanocellulose.

2. METHODOLOGY

2.1. Chemicals

In this research, a variety of chemicals were used, including sodium hydroxide (NaOH, 97%, HIMEDI), hydrogen peroxide (H_2O_2, 6%, SAMA PHARMA), sodium hypochlorite (NaOCl, 5.5%, UCL, Yemen), and ethanol (C_2H_5OH, 98%, LOBA CHEMIE, INDIA). Other chemicals used were lead nitrate (Pb $(NO_3)_2$) and cadmium nitrate Cd ($(NO_3)_2{\cdot}4H_2O$) provided by LOBA CHEMIE PVT. LTD. Additionally, acetic acid (CH_3COOH, 100%, LOBA CHEMIE, INDIA), hydrochloric acid (HCl, 35%, MERCK, GERMANY), sulfuric acid (H_2SO_4, 98%, MERCK, GERMANY), and Nitric Acid (HNO_3, 67%, MERCK, GERMANY). The analytical reagent grade chemicals were used without any additional purification processes. Deionized water (DIW) was consistently utilized in all experiments.

2.2. Pre-treatment of Sample

The fibers were manually removed from waste banana pseudostem (BPs) sourced from a local plantation using a dehulling process. Subsequently, the fibers were immersed in tap water and subsequently in heated deionized water, followed by thorough washing to eliminate contaminants. The material was segmented into small pieces measuring between 1 to 3 cm and dehydrated at 105 °C in an oven (J.P. SELECTA, SAPAIN) until a stable weight was attained (Sultana et al., 2020).

2.3. Extraction of Nanocellulose (NC)

The NC extraction procedure adhered to the protocol established in the previously published work by Al-Dabash & Al-Kahali (2024).

2.3.1. Degumming Process

The isolated fibers were degummed by refluxing the sample on a hot plate for two hours in a 12% w/v sodium hydroxide solution. A two-hour treatment with a 1% w/v H_2O_2 solution ensued. The samples were subsequently neutralized with 1% v/v acetic acid and re-treated with 6% w/v sodium hydroxide, followed by 1% w/v hydrogen peroxide. Subsequent to neutralization, the fibers were washed thrice with heated distilled water. The fiber-to-solution ratio was sustained at 1:15 (1 g of fiber in 15 mL of solution). The fibers were further dried in an oven at 60 °C for

16 hours, followed by size reduction through grinding and sieving.

2.3.2. Delignification Process

The fiber sample was delignified by boiling in 2% wt/v Na2SO3 for 10 minutes, followed by bleaching in 5% wt/v NaOCl for 30 minutes on a hot plate with magnetic stirring at 500 rpm. Prior to bleaching, the pH of the NaOCl was modified to 4-5 by including 5% (v/v) CH_3COOH, maintaining a fiber-to-solution ratio of 1:10 (1 g of fibers in 10 mL of solution). The delignification process was conducted twice until the fibers were entirely white, followed by three washes with hot distilled water. Thereafter, the delignified fibers were immersed in a 17.5% w/v NaOH solution for one hour to yield pure cellulose. The mixture was neutralized with a 10% v/v CH_3COOH solution and subsequently washed many times with deionized water until the filtrate attained a pH of 7. Subsequently, the cellulose was rinsed with 95% v/v ethanol and dehydrated in an oven at 60 °C for 16 hours (Lacaran et al., 2021; Islam et al., 2021).

2.3.3. Acid Hydrolysis and Ultrasonication

Nanocellulose was generated from cellulose isolated from banana pseudostem fiber using acid hydrolysis and ultrasound treatment. Fifteen grams of cellulose powder were combined with 60% v/v H2SO4, maintaining a fiber-to-solution ratio of 1:10 (1 gram of cellulose for 10 mL of H_2SO_4). The mixture underwent hydrolysis at 45 °C for 90 minutes with continuous agitation via a magnetic stirrer at 500 rpm. The reaction was subsequently halted by introducing double the volume of cold deionized water (10 °C) and neutralizing to a pH of 6–7 using a 2% w/v sodium hydroxide solution. The suspension was sonicated at 1% w/v using an ultrasonic bath (MU 14 /50–60 kHz) for 90 minutes, followed by centrifugation (DENLEY BS400 Centrifuge) at 6000 rpm for 15 minutes multiple times with deionized water. The sample was subsequently desiccated in an oven at 80 °C for 48 hours (Sukyai et al., 2018; Merais et al., 2022; Onkarappa et al., 2020; Lacaran et al., 2021).

2.4. Characterization of Nanocellulose as an Adsorbent

The surface morphology and dimensional distribution of the NC were analyzed using two techniques. The initial method, employing the Bozzola Russell methodology (1999), utilized the TEM-JEOL JEM-100CX II. The second method utilized a TEM-JEOL JEM-1400 and implemented the sample dissolving and dispersion technique with distilled water. The Fourier transform infrared (FT-IR) technique was employed to ascertain the functional groups of the NC, utilizing a Perkin Elmer spectrometer (Model: Nicolet 380, Manufacturer: Thermo Fisher Scientific) over a wavelength range of 400 to 4000 cm^{-1}, with an accuracy of 4 cm^{-1}. The elements Carbon, Oxygen, and Sulphur were examined, demonstrating the purity of the NC by Energy Dispersive X-ray (EDX) analysis linked with the FEl-SEM apparatus (FEI Company, Hillsboro, Oregon, USA). The surface area and porosity of NC were assessed by Brunauer-Emmett-Teller analysis (Quantachrome NOVA touch LX2, Micromeritics, USA).

2.5. Batch Adsorption Experiments

The stock solutions of lead and cadmium (1000 mg/L) were formulated by dissolving 1.5985 g of $Pb(NO_3)_2$ and

2.7435 g of $Cd(NO_3)_2 \cdot 4H_2O$ in deionized water, respectively. Batch adsorption tests utilize 50 ml of solutions containing Pb^{2+} or Cd^{2+}. The pH level was modified utilizing (0.1 M) HCl or (0.1 M) NaOH. Mixing was conducted in a shaker incubator at 180 rpm and ambient temperature. The parameters affecting the adsorption process were examined, including pH (3 – 7), contact duration (20 – 100 minutes), starting metal ion concentration (10 – 50 mg/L), and adsorbent dosage (0.05 – 0.25 g). Following the specified reaction duration, the adsorbent was isolated from the solution via centrifugation (MCL-DM0412 Centrifuge) at 3000 rpm for 5 minutes (Birgani et al., 2022; Abiaziem et al., 2019). A control experiment was conducted without the use of an adsorbent to ascertain any potential analyte loss via mechanisms other than adsorption. The residual concentrations of Pb^{2+} and Cd^{2+} ions were quantified post-adsorption via Atomic Absorption Spectrophotometry (AAS) (Perkin Elmer Analyst 400 /USA) by comparing the observed absorbance to the relevant standard on the calibration curve.

2.5.1. Data Analysis

The removal (%) of metal ions in each experiment was determined by using Eq. (1) (Farias et al., 2023):

$$\text{Removal } (\%) = \frac{C_0 - C_t}{C_0} \times 100 \quad \text{..... (1)}$$

The determination of the adsorption capacity (q_t) has been conducted to quantify the concentration of the adsorbed metal ion per unit mass of the adsorbent material (mg/g) at a designated contact time (t), employing Eq. (2) (Vázquez-Guerrero et al., 2021):

$$q_t = \frac{(C_0 - C_t) \times V}{m} \quad \text{..... (2)}$$

The determination of the adsorption capacity (q_e) has been conducted to quantify the concentration of the adsorbed metal ion per unit mass of the adsorbent material (mg/g) at equilibrium, using Eq. (3) (Farias et al., 2023):

$$q_e = \frac{(C_0 - C_e) \times V}{m} \quad \text{..... (3)}$$

Where C_0, C_t, and C_e (mg/L), the initial concentration, the residual concentration at a time (t), and the equilibrium concentrations of heavy metal ions, respectively. V (L) refers to the volume of the solution containing the Pb^{2+} and Cd^{2+} ions, and m (g) is the mass of the NC adsorbent.

2.5.2. Adsorption Kinetic Study

The data collected from studying the impact of contact time on the adsorption process of Pb^{2+} and Cd^{2+} by NC were analyzed using linear regression of the pseudo-first-order (1st order) and pseudo-second-order (2nd order) models, respectively. These models were chosen due to their widespread use and acceptance in studies on heavy metal adsorption by biosorbents. They have previously been used by Birgani et al. (2022), Dehvari et al. (2021), and Abiaziem et al. (2019).

2.5.2.1. Pseudo-first-order kinetic model

The 1st order kinetic model, developed by Lagergren, is expressed by Eq. (4) (Rahman et al., 2021).

$$\mathrm{Log}\,(q_e - q_t) = \mathrm{Log}q_e - \left(\frac{k_1}{2.303}\right)t \quad \text{..... (4)}$$

By using Eq. (4), a plot of log (q_e−q_t) on y-axis versus time values (t) on x-axis will give a straight line of 1st order adsorption model with y-intercept of (log q_e) and a graph slope equals (-k_1/2.303).

2.5.2.2. Pseudo-second-order kinetic model

The 2nd order kinetic model is predicated on the assumption that the rate determining step involves chemi-adsorption (Ho et al., 1998). This model is represented in its linear Eq. (5) (Rahman et al., 2021):

$$\left(\frac{t}{q_t}\right) = \left(\frac{1}{k_2 q_e^2}\right) + \left(\frac{1}{q_e}\right)t \quad \text{..... (5)}$$

The graph of (t/q_t) on the y-axis against time (t) on the x-axis displays a linear relationship. This relationship can be used to determine second-order constants. The slope of the graph represents ($1/q_e$), while the y-intercept represents ($1/K_2q_e^2$).

Where q_t represents the adsorption capacity (mg/g) at a specific time (t) per unit weight of NC adsorbent, q_e is the adsorption capacity at equilibrium (mg/g), K_1 is the 1st order rate constant (1/min), and k_2 represents the 2nd order rate constant at equilibrium with a unit of (g/min.mg)

2.5.3. Adsorption Isotherm Study

The experimental data from a study on the effect of concentration on the adsorption process of Pb^{2+} and Cd^{2+} by NC was used to study the adsorption isotherm at room temperature using the Langmuir and Freundlich models. The experimental data for Pb^{2+} and Cd^{2+} were fitted to the isotherm models using linear regression equations. The models used in this study have been previously used in studying the adsorption process of heavy metal ions on biosorbents surfaces by Birgani et al. (2022), Dehvari et al. (2021), and Abiaziem et al. (2019).

2.5.3.1. Langmuir Isotherm Model

The Langmuir model characterizes the adsorption process as a monolayer on a homogeneous surface. This model can be linearly expressed by Eq. (6) (Foo & Hameed, 2010; Swenson & Stadie, 2019).

$$\frac{C_e}{q_e} = \frac{1}{K_L q_{max}} + \left(\frac{1}{q_{max}}\right)C_e \quad \text{..... (6)}$$

By using Eq. (6), a plot of (C_e/q_e) values versus C_e values can be created for each adsorption, allowing for the determination of the Langmuir isotherm parameters. The slope of the plot represents ($1/q_{max}$), while the y-intercept represents ($1/K_Lq_{max}$).

The Langmuir isotherm is significantly relied on by the dimensionless equilibrium parameter (R_L), which acts as a separation factor. It is expressed in Eq. (7) (Abiaziem et al., 2019).

$$R_L = \frac{1}{1+ K_L C_0} \quad \text{..... (7)}$$

Where: R_L describes the probability of the adsorption process. If $R_L > 1$, then the adsorption process would be unfavorable, and if $0 < R_L < 1$, then this corresponds to an energetically favorable adsorption process. Lastly, if $R_L = 0$, the adsorption process can be irreversible (Abiaziem et al., 2019).

2.5.3.2. Freundlich Isotherm Model

The Freundlich model characterizes the adsorption process as multilayered and heterogeneous in nature. This model can be represented mathematically by Eq. (8). (Chen et al., 2017; Appel, 1973).

$$\text{Log } q_e = \text{Log } K_F + \left(\frac{1}{n}\right) \text{Log } C_e \quad \text{..... (8)}$$

Depending on Eq. (8), a plot of log q_e on the y-axis versus log C_e on the x-axis can be used to detect the parameters for the Freundlich isotherm including log K_F as the plot y-intercept and slope is the (1/n) value.

2.5.4. Analysis of Statistical

The experiments and findings were reported as mean ± standard deviation (SD) and standard error (SE). Linear regression equations and Pearson's equation were employed to compute correlation coefficients (R^2) for evaluating the compatibility of the adsorption models with the data. Moreover, Origin was employed to generate figures and graphical representations for the analysis of adsorption.

3. RESULTS AND DISCUSSION

3.1. Characterization of Nanocellulose

3.1.1. TEM Characterization

As previously delineated (Al-Dabash & Al-Kahali, 2024), the initial method (Figure 1a) illustrates a fibrous mesh configuration formed by interlaced strands of nanocellulose (NC). The diameter and length of the nanofibrils were ascertained via image analysis (Image J) of TEM micrographs, utilizing a minimum of 200 nanofibrils. The mean diameter and length of NC fibers were 28.9 ± 16.2 nm and 166.2 ± 104.5 nm, respectively. The rise in deviations from the average length dimensions can be ascribed to the measurement of fibers from all TEM images obtained using the approach of Bozzola and Russell (1999) and the protocol of the Asyut Medical Unit. In this approach, water was eliminated by sequentially substituting the solution with 30%, 50%, 70%, and 90% aqueous ethanol, each for a duration of two hours. This led to slight variations in the dimensions of the photos and affected the standard deviation. Furthermore, spherical cellulose nanocrystals were detected in the second approach, as illustrated in Figure 1b. The mean diameter of the NC sphere was 37.23 ± 6.93 nm. The histogram of particle size distribution (Gaussian curve) for NC-A sphericals is presented in Figure 1c.

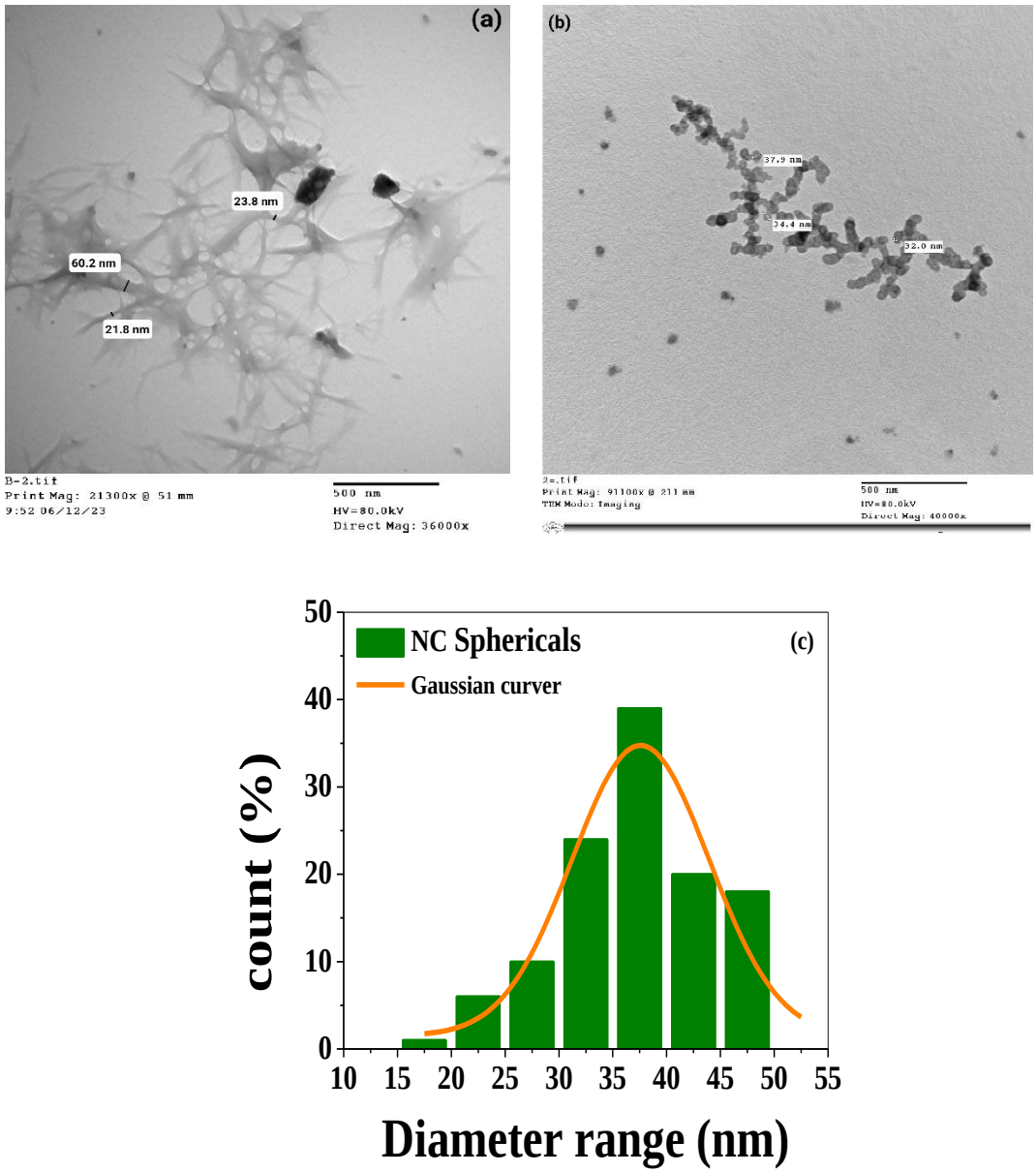

Figure 1. a, b) TEM images of NC and c) the diameter distribution of the NC spherical in image (b).

3.1.2. FTIR Characterization

Figure 2 displays the FT-IR spectra of NC extracted from banana pseudostem fiber. The peak at 3347.78 cm^{-1} indicates O-H stretching vibrations, while the notable spectral characteristics at 2894.55 cm^{-1} are associated with C-H bond stretching vibrations (Zhao et al., 2017; Evans et al., 2019). Additionally, specific signals related to cellulose are detected at 1640.50 cm^{-1} for C-H stretching, 1373.67 cm^{-1} for C-H bending vibration, 1324.22 cm^{-1} for CH_2 wagging, 1161.92 cm^{-1} for asymmetric vibration of C-O-C, 1116.76 cm^{-1} for stretching vibration of C-O-C pyranose ring, 1060.50 cm^{-1} for stretching vibration of C-O, and 898.25 cm^{-1} for symmetric vibration of C-H from β-glycosidic linkages (Chen et al., 2019; Samsudin et al., 2020; Moosavinejad et al., 2019). The peaks at 1276.70 cm^{-1}, 1241.99 cm^{-1}, and 611.80 cm^{-1} in the NC spectra are ascribed to S=O vibrations arising from the acid hydrolysis process. (Mamudu et al., 2023; Ramos-Vargas et al., 2020).

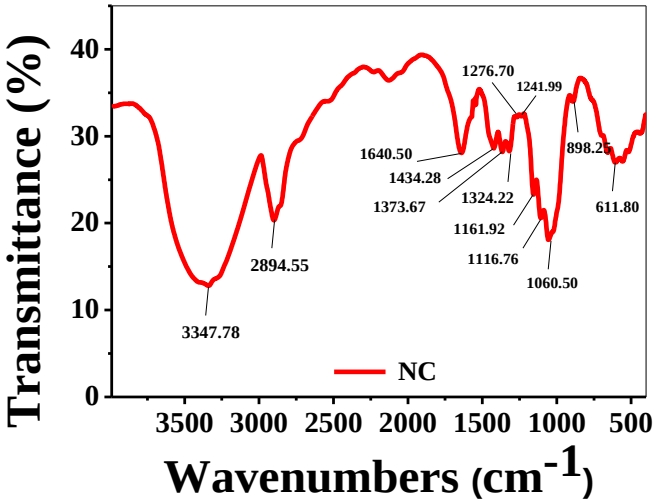

Figure 2. FTIR spectra of NC adsorbent

3.1.3 EDX Characterization

An first study was performed on a designated segment of NC utilizing energy-dispersive X-ray spectroscopy (EDX) in conjunction with field-emission scanning electron microscopy (FEI-SEM), as illustrated in Figure 3.

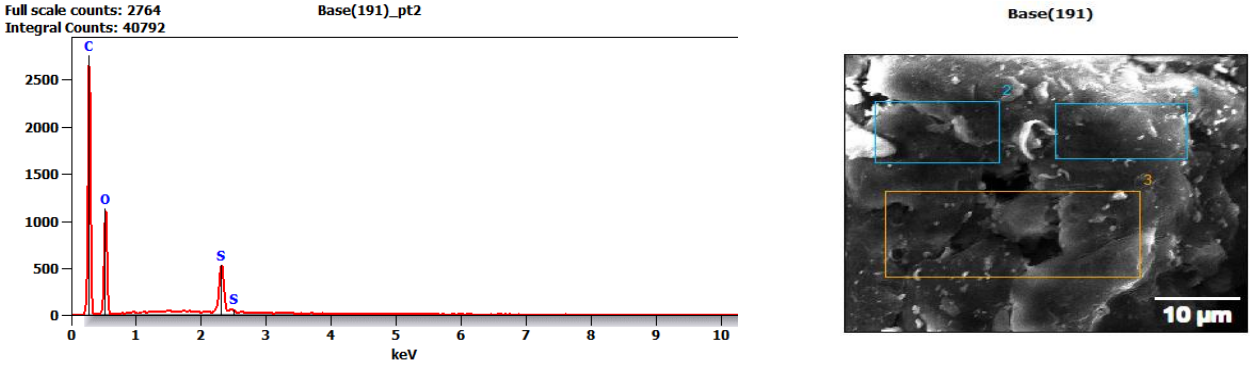

Figure 3. Chemical spectral analysis of NC by EDX associated with FEI-SEM

The average weight and atomic ratios of carbon (C), oxygen (O), and sulfur (S) on the surface of NC are shown in Table 1.

Table 1. Average ± SD the weight and atomic ratios of C, O and S on the surface of NC.

Ratio (%)	Carbon (C)	Oxygen (O)	Sulfur (S)
Weight	50.93 ± 3.56	44.47 ± 5.48	4.60 ± 2.39
Atom	56.23 ± 1.72	41.60 ± 1.87	2.17 ± 1.12

The EDX analysis revealed distinct peaks at approximately 0.20 keV, 0.50 keV, and (2.20 and 2.50 keV), which can be attributed to the energy levels of carbon, oxygen, and sulfur, respectively. The presence of sulfur in NC can primarily be attributed to the generation of anionic sulfate groups ($O\text{-}SO_3^-$) during the acid hydrolysis of sulfuric acid. This has occurred despite multiple washings of the suspension with DIW during centrifugation. The persistence of these sulfate groups can be attributed to their inherent resistance to removal, as they tend to adsorb onto the surface

of the nanocellulose (NC) during the acid hydrolysis process. The energy-dispersive X-ray (EDX) analysis corroborates the high purity levels of NC, aligning well with the Fourier-transform infrared (FTIR) spectra, which confirms the successful chemical treatments that have thoroughly eliminated hemicellulose and lignin. The findings align with prior study by Baraskar et al. (2023) and Dehvari et al. (2021), indicating that the NC surface possesses significant potential as an adsorbent for cationic contaminants. This is due to the presence of ionic O-SO^3- groups, as verified by EDX analysis, along with the dense anionic hydroxide groups on the surface of NC.

3.1.4. Brunauer-Emmett-Teller (BET) analysis

The surface area and porosity of the NC were determined using a nitrogen adsorption-desorption technique at 77.35 °K, as shown in (Figure 4). The average data obtained for NC for surface area (m^2/g), total pore volume (cm^3/g), and analyzer average pore size (nm) using Brunauer-Emmett-Teller (BET) analysis, are presented in Table 2.

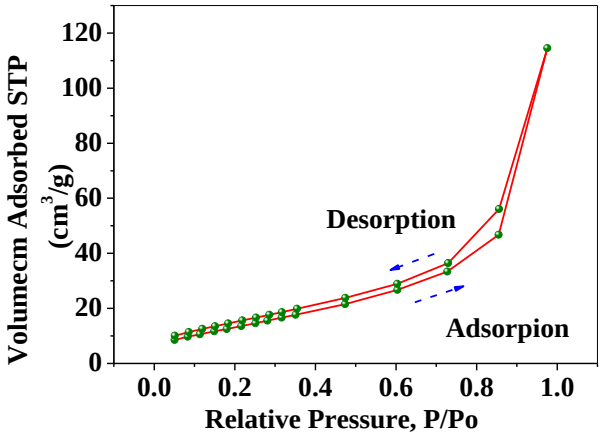

Figure 4. Adsorption and desorption isotherms in nitrogen gas for NC

Table 2. Comparison of adsorption surface area, total pore volume, and average pore size of NC with previous literature.

Feedstocks	Surface area (m^2/g)	Pore volume (cm^3/g)	Pore Diameter (nm)	Reference
Banana Pseudostem Fibers	52.3891	0.17752	6.77698	This study
Sugarcane Bagasse	1.8614	0.4277	9.4775	(Dehvari et al., 2021)
Wheat Straw	6.7	0.075	4.6	(Kaur & Pal, 2023)
Rice Husk	17.706	0.011	2.32589	(Baraskar et al., 2023)

3.2. Adsorption Studies

3.2.1. Effect of Some Parameters on Heavy Metal Ions Removal

3.2.1.1. Effect of pH Value

The pH of a solution is an important factor in determining the adsorption process, as it affects the surface charge of the adsorbent and the degree of ionization of the adsorbate.

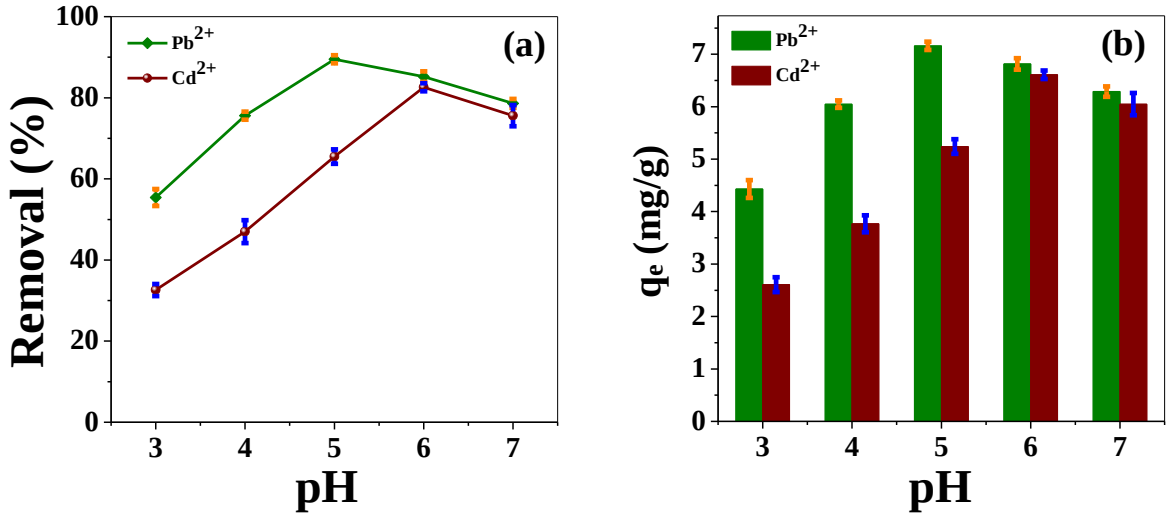

Figure 5. Effect of pH on a) removal (%) and b) adsorption capacity (q_e) of Pb^{2+} & Cd^{2+} onto the NC. Conditions: 0.125 g of NC; 50 mL ion solution at C_0 = 20 mg. L^{-1}.

Figure 5a & 5b shows the removal (%) and adsorption capacity (q_e) of Pb^{2+} and Cd^{2+} on the adsorbent surface at different pH levels (pH = 3 -7) in the aqueous solutions. It can be seen that the adsorption efficiency improves as the pH increases, reaching its highest point with Pb^{2+} at pH 5.0 and with Cd^{2+} at pH 6.0. However, the removal (%) diminishes as the pH continues to increase. The Pb^{2+} achieved the highest percentage at 89.5%, while cadmium achieved the highest percentage at 82.6%. The adsorption amounts at equilibrium for these ions were 7.160 mg/g and 6.608 mg/g, respectively. The adsorption capacity for Pb^{2+} and Cd^{2+} ions increases as the pH increases due to reduced competition between protons and the positively charged metal ions for binding sites on the surface of the NC. This is because at higher pH levels, there are fewer protons present to compete with the metal ions for binding sites. This allows for a greater amount of metal ions to bind to the surface of the NC, driven by electrostatic repulsion between the adsorbent surface and the ions in the solution (Dong et al., 2019). However, once the pH has been optimized for the NC, there is a decline in the percentage of adsorption for Pb^{2+} and Cd^{2+} ions. This is due to the formation of soluble hydroxide complexes, which reduces the efficiency of adsorption for these ions (Baraskar et al., 2023; Qiu et al., 2016).

3.2.1.2. Effect of Contact Time

Contact time significantly affects the removal efficiency of the adsorbent, as it impacts the equilibrium properties of the adsorption process. Therefore, the effect of time on the adsorption of Pb^{2+} and Cd^{2+} by NC was examined in batch mode for durations ranging from 20 to 100 minutes, at a temperature range of 25 ˚C.

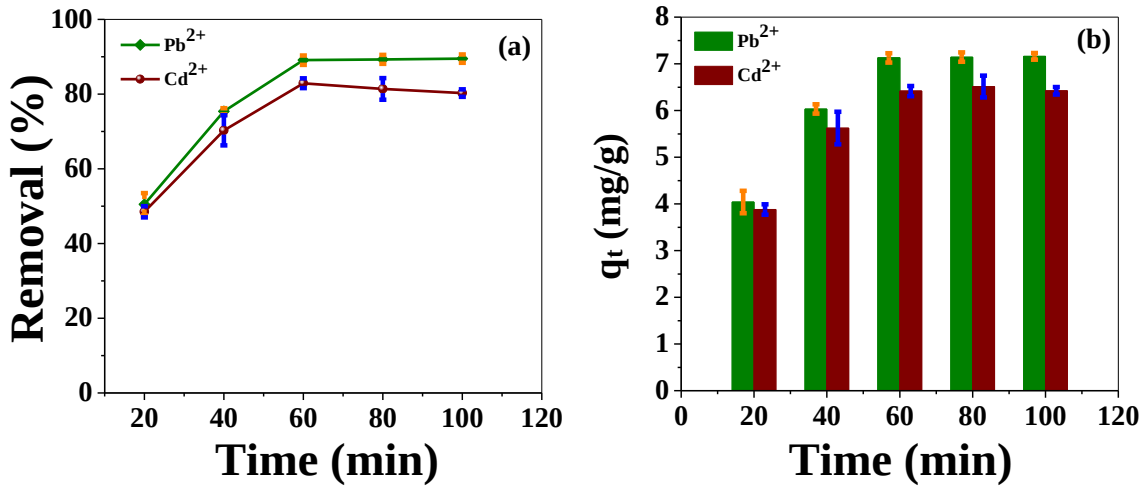

Figure 6. Effect of contact time on a) removal (%) and b) adsorption capacity (q_t) of Pb^{2+} & Cd^{2+} onto the NC. Conditions: 0.125 g of NC; 50 mL ion solution; C_0 = 20 mg. L^{-1} at the optimum pH values.

Figure 6a and 6b suggest that the equilibrium was reached after 60 min on NC, resulting in a removal of 89.1% for Pb^{2+} and 82.9% for Cd^{2+}. The amount of adsorbed for these ions at equilibrium was 7.128 mg/g and 6.416 mg/g, respectively. The results also show a significant increase in the adsorption percentage of both ions during the initial 40 minutes. The initial rapid adsorption is due to the availability of unoccupied regions on the adsorbent surface, allowing for greater acceptance of ions (Saini et al., 2019). However, as the surface becomes saturated, these locations become unavailable over time, resulting in a slower adsorption percentage (Birgani et al., 2022). Therefore, a contact time of 60 min was determined to be the optimal duration for the adsorption of Pb^{2+} and Cd^{2+} in aqueous solutions onto NC.

3.2.1.3. Effect of Metal Ion Concentration

The impact of metal ion concentration on adsorption is a crucial factor in adsorption research, as it can offer a valuable understanding of the correlation between the initial mineral ion concentration and maximum adsorption capacity (q_{max}). In this study, the concentrations of Pb^{2+} and Cd^{2+} were examined between 10-50 mg/L to investigate their effects in batch mode.

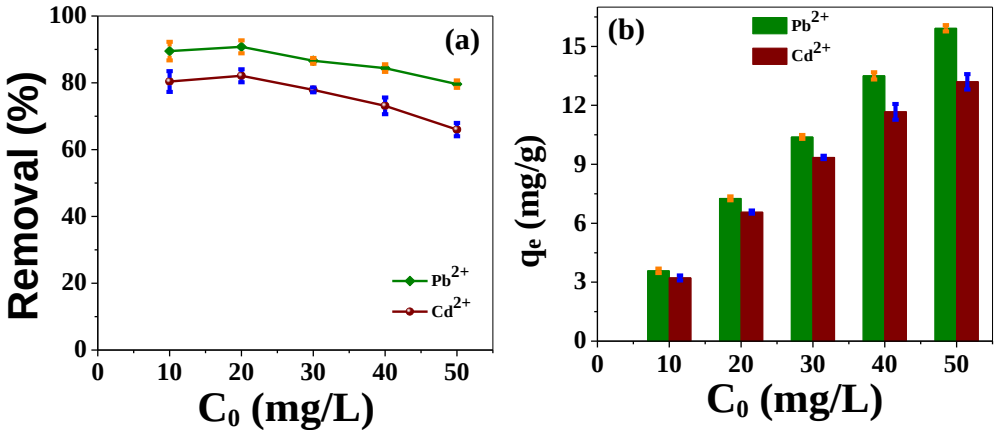

Figure 7. Effect of initial concentration on a) removal (%) and b) adsorption capacity (q_e) of Pb^{2+} & Cd^{2+} on the NC. Conditions: 0.125 g of NC; 50.0 mL ion solution; at optimal conditions for pH and contact time.

In Figure 7a & 7b, it can be observed that the removal (%) of Pb^{2+} and Cd^{2+} on NC decreases from 90.8 % to 79.3 % and 82.1 % to 66.0 %, respectively, as the concentration of metal ions increases from 10-50 mg/L. At a concentration of 10 mg/L, the percentage for Pb^{2+} and Cd^{2+} is 90.8 % and 82.1%, respectively, due to the presence of numerous active sites on the surface of the adsorbent (Kebede et al., 2018). However, as the concentration increases, these active sites become saturated with metal ions, resulting in a decrease in the adsorption of Pb^{2+} and Cd^{2+}. In contrast, the adsorption capacity of NC for Pb^{2+} and Cd^{2+} increases from 3.5800 to 15.9200 mg/g and 3.2160 to 13.200 mg/g, respectively. This is consistent with previous studies (Birgani et al., 2022; Dehvari et al., 2021; Abiaziem et al., 2019; Kardam et al., 2014). Based on these results, a concentration of 20 mg/L was determined to be the optimal concentration for the adsorption of Pb^{2+} and Cd^{2+} on NC from aqueous solutions.

3.2.1.4. Effect of Adsorbent Dose

The impact of the quantity of adsorbent NC on the adsorption of Pb^{2+} and Cd^{2+} ions was investigated under optimal conditions of pH, contact time, and initial concentration, using varying dose of adsorbent material ranging between (0.05 - 0.25 g). These experiments were conducted at room temperature, and the results obtained were documented in Figure 8a & 8b.

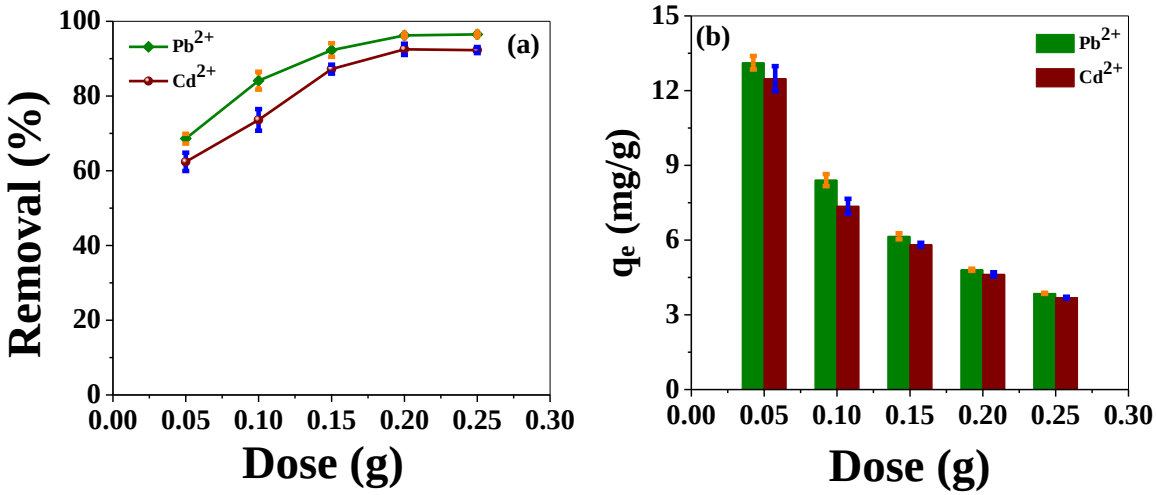

Figure 8. Effect of NC dose on a) the removal (%) and b) the adsorption capacity (q_e) of Pb^{2+} and Cd^{2+} onto the NC. Conditions: 50.0 mL Cd^{2+} solution at optimal conditions for pH, contact time, and initial concentration.

Based on the results in Figure 8a & 8b, the NC optimal amount of adsorption of Pb^{2+} and Cd^{2+} from aqueous solutions at optimum conditions (pH, contact time, and initial concentration) was found to be 0.20 g/50 mL. The removal (%) of lead and cadmium ions was 96.2% and 92.5%, respectively. The adsorbed amounts of Pb and Cd ions at equilibrium were 4.810 mg/g and 4.625 mg/g, respectively. At the low dosage of 0.05 g, the adsorption of heavy metal ions is restricted due to the limited number of active binding sites available. However, as the dose increases, the adsorption efficiency improves due to the availability of additional binding sites. Once the optimal dose of 0.20 g is achieved, the adsorption efficiency remains constant because the surface sites become saturated and unable to adsorb further ions. This phenomenon occurs due to the overlapping and crowding of adsorbed molecules, which hinders the adsorption process (Yousefi et al., 2018). It is also noted from the results that lead ions have a higher selectivity for

adsorption on the surface of NC compared to cadmium, this is consistent with the results of previous studies (Birgani et al., 2022; Baraskar et al., 2023; Kardam et al., 2014).

3.2.2. *Investigation of Adsorption Kinetic Models*

In this study, the adsorption kinetics of Pb^{2+} and Cd^{2+} on the NC adsorbent were determined using the 1st order Eq. (4) and the 2nd order Eq. (5). The corresponding graphs for these models can be seen in Figure 9, and a summary of the results is shown in Table 3.

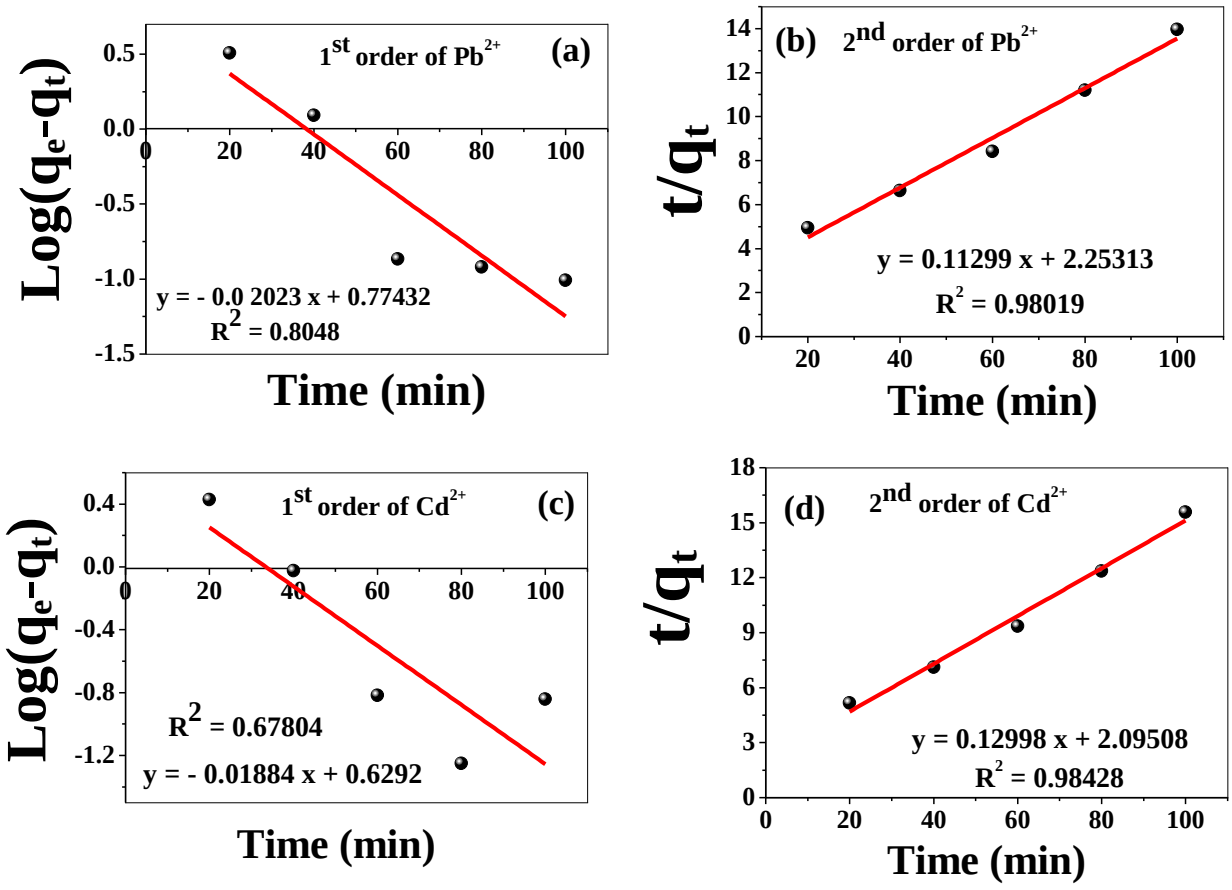

Figure 9. Linear relationship of adsorption kinetic models for Pb^{2+} ions (a, b), and for Cd^{2+} ions (c, d) on NC.

The analysis of the results summarized in (Tables 3) reveals that the correlation coefficient values (R^2) for the adsorption of Pb^{2+} and Cd^{2+} onto the surface of NC, as estimated by the 1st order model, are lower than the R^2 values obtained for the same ions when adsorbed onto NC compared to the 2nd order model. Additionally, a notable difference was observed between the practical adsorption amount at equilibrium ($q_{e\ exp.}$) and the theoretical adsorption quantity ($q_{e\ cal.}$) for both Pb^{2+} and Cd^{2+} using the 1st order model noted in the R^2 value, while note a convergence between the experimentally determined adsorption capacity ($q_{e\ exp.}$) and the theoretically calculated adsorption capacity ($q_{e\ cal.}$) at equilibrium for Pb^{2+} and Cd^{2+} using the 2nd order model as shown in the value of R^2. Consequently, it can be inferred that the 2nd order model is more suitable than the 1st order model for describing the adsorption of Pb^{2+} and Cd^{2+} onto the surface of NC. These results are consistent with the findings of previous studies, which have shown the dominance of the 2nd order during the adsorption process of Pb^{2+} or Cd^{2+} ions or both on the surface of NC extracted from plant

biomass waste by the acid hydrolysis method, including the studies of Baraskar et al. (2023), Kaur et al. (2020), Kara et al. (2021), and Dehvari et al. (2021). However, these results contrast with other studies where the 1st order was found to be more applicable during the adsorption process, as such the study by Birgani et al. (2022), Kaur & Pal (2023), and Ramos-Vargas et al. (2020).

Table 3. Summary of calculated parameters for 1st order and 2nd order kinetic models for the adsorption of Pb^{2+} and Cd^{2+} on NC.

kinetic Model	Parameters	Metal ions	
		Pb^{2+}	Cd^{2+}
	$q_{e\ exp.}$(mg/g)	7.26400	6.65600
Pseudo-first-order	k_1(1/min)	0.04658	0.04339
	$q_{e\ cal.}$ (mg/g)	5.9473	4.25790
	R^2	0.8048	0.67804
Pseudo-second-order	k_2 (g/mg.min)	0.0057	0.0081
	$q_{e\ cal.}$ (mg/g)	8.85030	7.69350
	R^2	0.98019	0.98428

3.2.3. *Investigation on Adsorption Isotherms Models*

The adsorption isotherms of Pb and Cd ions were determined using the Langmuir and Freundlich models, as shown in Eq. (6) and (8). Figure 10 shows the Langmuir and Freundlich diagrams for the adsorption of Pb^{2+} and Cd^{2+} on NC, respectively.

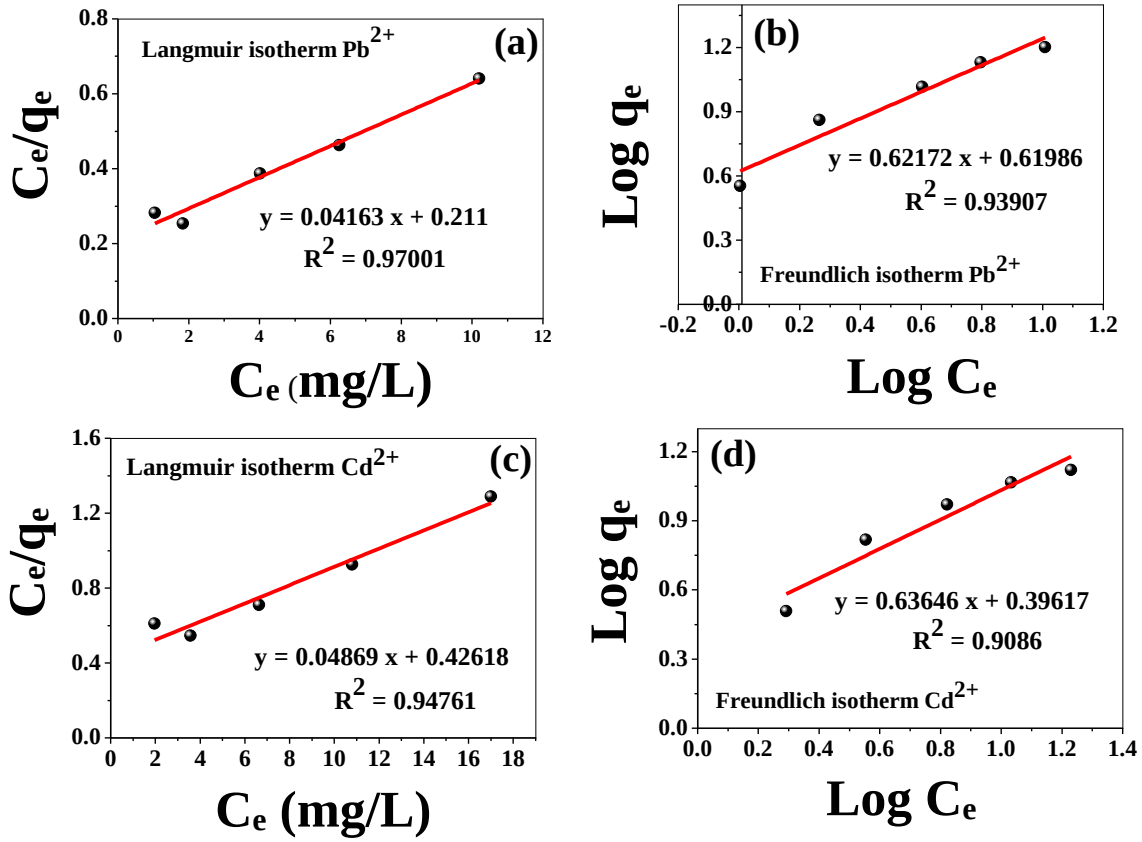

Figure 10. Linear relationship of adsorption isotherm models of Pb^{2+} (a, b) and Cd^{2+} (c, d) on the NC at room temperature.

The presented parameters of isotherm models and correlation coefficient (R^2) values in Table 4, for the adsorption of Pb^{2+} and Cd^{2+} using the Langmuir and Freundlich isotherm models. The results indicate that the Langmuir model accurately fits the experimental data and is the most suitable for describing the adsorption process of Pb^{2+} and Cd^{2+} on the surfaces of the NC adsorbent. This is evident from the high correlation coefficient values (R^2) and separation factor (R_L) shown in Table 4. The R_L values obtained from Eq. (7) at equilibrium for Pb^{2+} and Cd^{2+} were 0.20 and 0.30, respectively. These values suggest favorable adsorption ($0 < R_L < 1$) according to the Langmuir model, which assumes homogeneous adsorption sites on the adsorbent.

A similar trend can be observed in the results related to adsorption onto NC, which aligns with the research conducted by Birgani et al. (2022) and Kardam et al. (2014). These studies analyzed the adsorption behavior of Pb^{2+} and Cd^{2+} ions in aqueous solutions on the surface of NC, derived from plant biomass waste through acid hydrolysis, using the Langmuir and Freundlich models. The findings showed that the Langmuir model provided the best fit for the adsorption process. However, the outcomes of other investigations, such as those by Dehvari et al. (2021) and Kaur et al. (2020), differ from these findings as they identified the Freundlich model as the most appropriate for describing the adsorption process.

Table 4. The parameters calculated summary of the Langmuir and Freundlich isotherm model for Pb^{2+} and Cd^{2+} on NC at 25 ˚C.

Metal Ion	Langmuir				Freundlich		
	q_{max} (mg/g)	K_L (L/mg)	R^2	R_L	n	K_F	R^2
Pb^{2+}	24.02	0.1973	0.97001	0.20	1.6084	4.1673	0.93307
Cd^{2+}	20.54	0.1142	0.94761	0.30	1.5712	2.4899	0.9086

The adsorption capacity (q_{max}) for Pb^{2+} and Cd^{2+} ions according to the Langmuir isotherm model was determined to be 24.02 mg/g and 20.34 mg/g, respectively. In comparison with other adsorbents manufactured from natural materials, based on these results, the nanocellulose produced in this work showed competitive performance (Table 5).

Table 5. A Comparison between the q_{max} of prepared NC other adsorbents manufactured from natural biomaterials reported from literature sources.

Adsorbent Type	Heavy Metal Ion	q_{max} (mg/g)	Reference
NC Banana (*Musa SPP.*) Pseudostem fibers	Pb^{2+} Cd^{2+}	24.02 20.54	This work
NC Rice (*Oryza sativa L.) husk*	Cd^{2+} Pb^2	3.64 3.45	(Baraskar et al., 2023)
NC Waste Sugarcane Bagasse (*Saccharum officinarum L.*)	Cd^{2+}	20	(Dehvari et al., 2021)
NC Cassava (*Manihot esculenta*) Peel	Pb^{2+}	14.43	(Abiaziem et al., 2019)
Commercial activated carbon	Cd^{2+}	10.3	(Hydari et al., 2012)
Peels of banana	Pb^{2+} Cd^{2+}	5.71 2.18	(Anwar et al., 2010)
Pine bark modified with NaOH	Pb^{2+} Cd^{2+}	11.40 10.5	(Argun et al., 2009)

4. CONCLUSION

The EDX analysis revealed the presence of sulfur on the surface of the Nanocellulose (NC), which is attributed to the acidic hydrolysis resulting in the incorporation of sulfate groups ($O\text{-}SO_3^-$) into the NC. Additionally, the EBT analysis showed that the NC has a surface area of 52.3891 m^2/g. The presence of $O\text{-}SO_3^-$ groups and the increase in surface area of NC enhance its ability to remove chemical pollutants from aqueous solutions. The adsorption results indicate that NC has good adsorption efficiency to some extent of lead and cadmium ions, making the technique a promising solution for water treatment, particularly industrial wastewater. Moreover, the addition of other nano-particles or modification procedures to the NC surface could potentially enhance the efficiency and effectiveness in treating heavy metal pollution. The use of biomass from the banana pseudostem offers a readily available and sustainable solution for managing waste and utilizing it in various applications, including improving the quality of water resources.

Current and future research on NC focuses on its potential and properties as a promising material for treating water pollution. Based on our study, we propose the following recommendations:

- Evaluate the potential of extracted NC from banana biomass waste as a material with significant promise in various applications, including treating water contamination with heavy metals and other chemical pollutants.
- Expand research efforts on NC to investigate its capacity for removing organic dyes, specifically applying it to wastewater samples from the textile industry for further analysis.
- Investigate the recovery of the NC and its reuse in the removal of heavy metals and organic dyes, aiming to evaluate its efficiency and the number of recovery cycles achievable while also considering feasibility studies.
- Utilize biomass residues from other locally abundant plants to extract NC, employing a cost-effective and environmentally sustainable approach, while studying its properties and potential applications in treating water pollution.

ACKNOWLEDGMENTS

I express my profound gratitude to the University of Aden and the University of Science and Technology, along with the Microscopy and Chemistry Departments at the Cairo University Research Park (CURP). Additionally, I extend my appreciation to the Molecular Biology and Physics Departments at the Faculty of Science, Assiut University, Egypt, and the Diamond Research Laboratory in Cairo, Egypt, for the facilities granted to us to complete the research work.

AUTHOR CONTRIBUTIONS

The 1st author performed sampling, laboratory analysis, and manuscript writing. The 2nd author contributed to manuscript writing, review, and editing.

FUNDINGS

Not applicable.

DATA AVAILABILITY

Not applicable.

COMPETING INTEREST

The authors declare that they have known competing financial interests or personal relationships that could have appeared to influence the work reported in this paper.

COMPLIANCE OF ETHICAL STANDARDS

Not applicable.

SUPPLEMENTARY MATERIAL

Not applicable.

REFERENCES

Abiaziem, C.V., Williams, A.B., Inegbenebor, A.I., Onwordi, C.T., Ehi-Eromosele, C.O., & Petrik, L.F. (2019). Adsorption of lead ion from aqueous solution unto cellulose nanocrystal from cassava peel. *Journal of Physics. Conference Series, 1299*(1), 012122. http://dx.doi.org/10.1088/1742-6596/1299/1/012122

Ahmad, R., & Mirza, A. (2018). Facile one pot green synthesis of Chitosan-Iron oxide (CS-Fe_2O_3) nanocomposite: Removal of Pb (II) and Cd (II) from synthetic and industrial wastewater. *Journal of Cleaner Production, 186,* 342–352. https://doi.org/10.1016/j.jclepro.2018.03.075

Akhtar, M., Sarfraz, M., Ahmad, M., Raza, N., & Zhang, L. (2025). Use of low-cost adsorbent for waste water treatment: Recent progress, new trend and future perspectives. *Desalination and Water Treatment, 321,* 100914. https://doi.org/10.1016/j.dwt.2024.100914

Al-Dabash, B. M., & Al-Kahali, M. S. (2024). Morphological and structural characterization of nanocellulose extracted from banana pseudostem waste. *Electronic Journal of University of Aden for Basic and Applied Sciences, 5*(4), 531-542. http://dx.doi.org/10.47372/ejua-ba.2024.4.410

Ali, A. (2017). Removal of Mn (II) from water using chemically modified banana peels as efficient adsorbent. *Environmental Nanotechnology, Monitoring & Management*, *7*(1), 57-63. http://dx.doi.org/10.1016/j.enmm.2016.12.004

Anwar, J., Shafique, U., Waheed-uz-Zaman, Salman, M., Dar, A., & Anwar, S. (2010). Removal of Pb(II) and Cd(II) from water by adsorption on peels of banana. *Bioresource Technology,* 101(6), 1752–1755. https://doi.org/10.1016/j.biortech.2009.10.021

Appel, J. (1973). Freundlich's adsorption isotherm. *Surface Science, 39* (1), 237–244. https://doi.org/10.1016/0039-6028(73)90105-2

Argun, M. E., Dursun, S., & Karatas, M. (2009). Removal of Cd (II), Pb (II), Cu (II) and Ni (II) from water using modified pine bark. *Desalination,* 249 (2), 519–527. https://doi.org/10.1016/j.desal.2009.01.020

Ariffin, N., Abdullah, M. M. A. B., Mohd Arif Zainol, M. R. R., Murshed, M. F., Hariz-Zain, Faris, M. A., & Bayuaji, R. (2017). Review on Adsorption of Heavy Metal in Wastewater by Using Geopolymer. *MATEC Web of Conferences*, 97 (1), 01023. https://doi.org/10.1051/matecconf/20179701023

Aziz, T., Haq, F., Farid, A., Kiran, M., Faisal, S., Ullah, A., & Show, P. L. (2023). Challenges associated with cellulose composite material: Facet engineering and prospective. *Environmental Research, 13,* (26), 115429. https://doi.org/10.1016/j.envres.2023.115429

Baraskar, P. N., Samant, R. A., & Gurav, V. L. (2023). Removal of heavy metal ions using nano-cellulose prepared from rice husk: validation by differential pulse voltammetry. *Analytical Chemistry Letters, 13* (4), 432–450. http://dx.doi.org/10.21203/rs.3.rs-3279156/v1

Birgani, A. S., Talaeipour, M., Hemmasi, A., Bazyar, B., & Larijani, K. (2022). Removal of heavy metal ions using cellulose nanocrystals and succinic anhydride-modified cellulose nanocrystals prepared from bleached soda bagasse pulp. *BioResources, 3* (17), 4886-4904. https://doi.org/10.15376/biores.17.3.4886-4904

Blasi, A., Verardi, A., Lopresto, C. G., Siciliano, S., & Sangiorgio, P. (2023). Lignocellulosic Agricultural Waste *Valorization to Obtain Valuable Products: An Overview. Recycling, 8(*4), 61. https://doi.org/10.3390/recycling8040061

Bozzola, J.J., & Russell, L.D. (1999) Electron Microscopy: Principles and Techniques for Biologists. *Jones and Bartlett, Bosto*n, 670 p. https://www.scirp.org/reference/ReferencesPapers?ReferenceID=1368539

Briffa, J., Sinagra, E., & Blundell, R. (2020). Heavy metal pollution in the environment and their toxicological effects on humans. *Heliyon, 6* (9), e04691. https://doi.org/10.1016/j.heliyon.2020.e04691

Chen, K., He, J., Li, Y., Cai, X., Zhang, K., Liu, T., … Liu, J. (2017). Removal of cadmium and lead ions from water by sulfonated magnetic nanoparticle adsorbents. *Journal of Colloid and Interface Science, 194* (15), 307–316. https://doi.org/10.1016/j.jcis.2017.01.082

Chen, Y.W., Hasanulbasori, M.A., Chiat, P.F., & Lee, H.V. (2019). Pyrus pyrifolia fruit peel as sustainable source for spherical and porous network based nanocellulose synthesis via one-pot hydrolysis system. *International Journal of Biological Macromolecules, 123* (18), 1305-1319. https://doi.org/10.1016/j.ijbiomac.2018.10.013

Dehvari, M., Jamshidi, B., Jorfi, S., Pourfadakari, S., & Skandari, Z. (2021). Cadmium removal from aqueous solution using cellulose nanofibers obtained from waste sugarcane bagasse (SCB): isotherm, kinetic, and thermodynamic studies. *Desalination And Water Treatment, 221*(5): 218-228. https://doi.org/10.5004/dwt.2021.27060

Dong, J., Du, Y., Dudu, R., Shang, Y., Zhang, S. and Han, R. (2019). Adsorption of copper ion from solution by polyethyleneimine modified wheat straw. *Bioresource Technology Reports, 6*, 96-102.http://dx.doi.org/10.1016/j.biteb.2019.02.011.

Evans SK., Wesley O.N., Nathan O., Moloto M.J. (2019) Chemically purified and its nanocrystals from sugarcane bagasse isolation and characterization, *Heliyon, 5*(10), e02635. https://doi.org/10.1016/j.heliyon.2019.e02635..

Farias, K.C.S., Guimarães, R.C.A., Oliveira, K.R.W., Nazário, C.E.D., Ferencz, J.A.P., & Wender, H. (2023). Banana peel powder biosorbent for removal of hazardous organic pollutants from wastewater. *Toxics, 11*(8), 664. https://doi.org/10.3390/toxics11080664

Foo, K.Y., & Hameed, B.H. (2010). Insights into the modeling of adsorption isotherm systems. *Chemical Engineering Journal, 156*(1), 2–10. https://doi.org/10.1016/j.cej.2009.09.013.

Grishkewich, N., Mohammed, N., Tang, J., & Tam, K.C. (2017). Recent advances in the application of cellulose nanocrystals. *Current Opinion in Colloid & Interface Science, 29*, 32-45. https://doi.org/10.1016/j.cocis.2017.01.005

Ho, Y.S. McKay G. (1998). Sorption of dye from aqueous solution by peat. *Chemical Engineering Journal, 70*(2), 115-124.https://doi.org/10.1016/S0923-0467(98)00076-1.

Hydari, S., Sharififard, H., Nabavinia, M., & Parvizi, M.r. (2012). A comparative investigation on removal performances of commercial activated carbon, chitosan biosorbent and chitosan/activated carbon composite for cadmium. *Chemical Engineering Journal,* 193-194, 276–282. https://doi.org/10.1016/j.cej.2012.04.057.

Isawi, H. (2020). Using Zeolite/Polyvinyl alcohol/sodium alginate nanocomposite beads for removal of some heavy metals from wastewater. *Arabian Journal of Chemistry, 13*(6), 5691-5716. https://doi.org/10.1016/j.arabjc.2020.04.009

Islam, Md. M., Islam, Md. S., Maniruzzaman, Mohd., Haque, Md. M.-U., & Mohana, A.A. (2021). Banana rachis CNC/Clay composite filter for dye and heavy metals adsorption from industrial wastewater. *Engineering Science & Technology, 32*(2), 44–56. https://doi.org/10.37256/est.222021817

Kara, H.T., Anshebo, S.T., & Sabir, F.K. (2021). Adsorptive removal of Cd (II) ions from wastewater using maleic anhydride nanocellulose. *Journal of Nanotechnology, 52*(2), 1-15. https://doi.org/10.1155/2021/9966811

Kardam, A., Raj, K.R., Srivastava, S., & Srivastava, M.M. (2014). Nanocellulose fibers for biosorption of cadmium, nickel, and lead ions from aqueous solution. *Clean Technologies and Environmental Policy, 2*, 385-393. https://doi.org/10.1007/s10098-013-0634-2

Kaur, M., & Pal, J. (2023). Evaluation of efficiency of Wheat straw nanocellulose as nanoadsorbent for the removal of divalent copper, lead and zinc from aqueous solution. *Carbohydrate Polymer Technologies and Applications, 6*(1), 100350. https://doi.org/10.1016/j.carpta.2023.10035

Kaur, M., Kumari, S., & Sharma, P. (2020). Removal of Pb (II) from aqueous solution using nanoadsorbent of Oryza sativa husk: Isotherm, kinetic and thermodynamic studies. *Biotechnology Reports, 25*(6), e00410. https://doi.org/10.1016/j.btre.2019.e00410

Kebede, T.G., Mengistie, A.A., Dube, S., Nkambule, T.T.I. and Nindi, M.M. (2018). Study on adsorption of some common metal ions present in industrial effluents by *Moringa stenopetala* seed powder. *Journal of Environmental Chemical Engineering,* 6(1), 1378-1389. http://dx.doi.org/10.1016/j.jece.2018.01.012

Kim, J.S., Lee, Y.Y., & Kim, T.H. (2016). A review on alkaline pretreatment technology for bioconversion of

lignocellulosic biomass. *Bioresource Technology, 199*(1), 42-48. https://doi.org/10.1016/j.biortech.2015.08.085

Lacaran, J. V. T., Narceda, R. J., Bilo, J. a. V., & Leaño, J. L., Jr. (2021). Citric acid crosslinked nanofibrillated cellulose from banana (*Musa Acuminata* X balbisiana) Pseudostem for adsorption of Pb^{2+} and Cu^{2+} in aqueous solutions. *Cellulose Chemistry and Technology, 55*(3-4), 403-415. https://doi.org/10.35812/cellulosechemtechnol

Mahfoudhi, N.& Boufi, S. (2017). Nanocellulose as a novel nanostructured adsorbent for environmental remediation: a review. *Cellulose, 24*(3),1171–1197. https://doi: 10.1007/s10570-017-1194.

Mamudu, U., Hussin, M.R., Santos, J.H., & Lim, R.C. (2023). Synthesis and Characterisation of sulfated-nanocrystalline cellulose in epoxy coatings for corrosion protection of mild steel from sodium chloride solution. *Carbohydrate Polymer Technologies and Applications, 5*(2), 100306. https://doi.org/10.1016/j.carpta.2023.100306

Merais, M.S., Khairuddin, N., Salehudin, M.H., Siddique, M.B.M., Lepun, P., & Chuong, W.S. (2022). Preparation and characterization of cellulose nanofibers from banana pseudostem by acid hydrolysis: Physico-chemical and thermal properties. *Membranes, 12*(5), 451. http://dx.doi.org/10.3390/membranes12050451.

Mitra, S., Chakraborty, A. J., Tareq, A.M., Emran, T.B., Nainu, F., Khusro, A., … Simal-Gandara, J. (2022). Impact of heavy metals on the environment and human health: Novel therapeutic insights to counter the toxicity. *Journal of King Saud University - Science, 34*(3), 101865. https://doi.org/10.1016/j.jksus.2022.101865

Mo, Y., Huang, X., Yue, M., Hu, L., & Hu, C. (2024). Preparation of nanocellulose and application of nanocellulose polyurethane composites. *RSC Advances, 14*(26), 18247–18257. https://doi.org/10.1039/d4ra01412j.

Moosavinejad SM., Madhoushi M., Vakili M., Rasouli. (2019) Evaluation of degradation in chemical compounds of wood in historical building using FTIR and FT-Raman vibrational spectroscopy. *Maderas Ciencia y Technologia, 21*(3), 381-392. https://doi.org/10.4067/S0718-221X2019005000310

Onkarappa, H.S., Prakash, G.K., Pujar, G.H., Rajith Kumar, C.R., Radha, V., & Betageri, V. S. (2020). Facile synthesis and characterization of nanocellulose from husk. *Polymer Composites, 41*(8), 3153-3159. https://doi.org/10.1002/pc.25606

Panchal, P., Ogunsona, E., & Mekonnen, T. (2018). Trends in advanced functional material applications of nanocellulose. *Processes, 7*(1), 10. https://doi.org/10.3390/pr7010010

Qiu, H., Yan, J., Lan, G., Liu, Y., Song, X., Peng, W. & Cui, Y. (2016). Removal of Cu2+ from wastewater by modified xanthan gum (XG) with ethylenediamine (EDA). *Royal Society of Chemistry Advances, 6*(86), 83226–83233.http://dx.doi.org/10.1039/C6RA11423G

Rafati Rahimzadeh, M., Rafati Rahimzadeh, M., Kazemi, S. & Moghadamnia, A.A. (2017). Cadmium toxicity and treatment: An update. *Caspian Journal of Internal Medicine, 8*(3), 135-145. https://doi: 10.22088/cjim.8.3.135

Rahman, M.L., Wong, Z.J., Sarjadi, M.S., Soloi, S., Arshad, S.E., Bidin, K., & Musta, B. (2021). Heavy metals removal from electroplating wastewater by waste fiber-based Poly(amidoxime) ligand. *Water, 13*(9), 1260.

https://doi.org/10.3390/w13091260

Ram, B., & Chauhan, G.S. (2018). New spherical nanocellulose and thiol-based adsorbent for rapid and selective removal of mercuric ions. *Chemical Engineering Journal*, 331, 587-596. http://dx.doi.org/10.1016/j.cej.2017.08.128

Ramos-Vargas, S., Huirache-Acuña, R., Rutiaga-Quiñones, J.G., & Cortés-Martínez, R. (2020). Effective lead removal from aqueous solutions using cellulose nanofibers obtained from water hyacinth. *Water Supply, 20*(7), 2715–2736. http://dx.doi.org/10.2166/ws.2020.173

Reshmy, R., Philip, E., Madhavan, A., Pugazhendhi, A., Sindhu, R., Sirohi, R., Awasthi, M. K., Pandey, A., & Binod, P. (2022). Nanocellulose as green material for remediation of hazardous heavy metal contaminants. *Journal of Hazardous Materials, 424*, 127516. https://doi.org/10.1016/j.jhazmat.2021.127516

Saini, S., Kanoria, J. and Kaur, I. (2019). A comparative study for removal of cadmium (II) ions using unmodified and NTA-modified *Dendrocalamus strictus* charcoal powder. *Journal of Environmental Health Science and Engineering, 17*(1), 259-272. https://doi.org/10.1016/j.arabjc.2018.06.003

Samsudin N.A., Low F.W., Yusoff Y., Shakeri M., Tan X.Y., Lai C.W., Asim N., Oon C.S., Newaz K.S., Tiong S.K., Amin N. (2020) Effect of temperature on synthesis of cellulose nanoparticles via ionic liquid hydrolysis process. *Journal of Molecular Liquids, 308*, 113030. https://doi.org/10.1016/j.molliq.2020.113030

Sukyai, P., Anongjanya, P., Bunyahwuthakul, N., Kongsin, K., Harnkarnsujarit, N., Sukatta, U., & Chollakup, R. (2018). Effect of cellulose nanocrystals from sugarcane bagasse on whey protein isolate-based films. *Food Research International, 107* (4): 528–535. https://doi.org/10.1016/j.foodres.2018.02.052.

Sultana, T., Sultana, S., Nur, H.P., & Khan, M.W. (2020). Studies on mechanical, thermal and morphological properties of betel nut husk nano cellulose reinforced biodegradable polymer composites. *Journal of Composites Science, 4*(3), 83. https://doi.org/10.3390/jcs4030083

Swenson, H., & Stadie, N.P. (2019). Langmuir's Theory of Adsorption: A Centennial Review. *Langmuir, 35*(16), 5409–5426. https://doi.org/10.1021/acs.langmuir.9b00154

Tchounwou, P.B., Yedjou, C.G., Patlolla, A.K., & Sutton, D.J. (2012). Heavy Metal Toxicity and the Environment. In Luch A (Ed) Molecular, Clinical and Environmental Toxicology. Volume 3: Environmental Toxicology, Springer Basel, Basel. pp. 133–164. http://dx.doi.org/10.1007/978-3-7643-8340-4_6.

Tshikovhi, A., Mishra, S.B., & Mishra, A.K. (2020). Nanocellulose-based composites for the removal of contaminants from wastewater. *International Journal of Biological Macromolecules, 152*, 616-632. https://doi.org/10.1016/j.ijbiomac.2020.02.221

Vázquez-Guerrero, A., Cortés-Martínez, R., Alfaro-Cuevas-Villanueva, R., Rivera-Muñoz, E., & Huirache-Acuña, R. (2021). Cd (II) and Pb (II) adsorption using a composite obtained from *Moringa oleifera* Lam. cellulose nanofibrils impregnated with iron nanoparticles. *Water, 13*(1), 89. https://doi.org/10.3390/w13010089

Wang, G., Zhang, J., Lin, S., Xiao, H., Yang, Q., Chen, S., ... & Gu, Y. (2020). Environmentally friendly

nanocomposites based on cellulose nanocrystals and polydopamine for rapid removal of organic dyes in aqueous solution. *Cellulose*, *27*, 2085-2097. https://doi.org/10.1007/s10570-019-02944-6

Yadav, M., Singh, G., & Jadeja, R.N. (2021). Physical and chemical methods for heavy metal removal. In: Singh, P., Singh, R., Singh, V.K., & Bhadouria, R (Eds) Pollutants and Water Management: Resources, Strategies and Scarcity, Wiley, New Jersey. pp. 377-397. https://doi.org/10.1002/9781119693635.ch15

Yousefi, T., Mohsen, M.A., Mahmudian, H.R., Torab-Mostaedi, M., Moosavian, M.A. & Aghayan, H. (2018). Removal of Pb (II) by modified natural adsorbent; Thermodynamics and kinetics studies. *Journal of Water and Environmental Nanotechnology, 3*(3), 265-272. https://doi.org/10.22090/jwent.2018.03.007

Zaini, H.M., Saallah, S., Roslan, J., Sulaiman, N.S., Munsu, E., Wahab, N.A., & Pindi, W. (2023). Banana biomass waste: A prospective nanocellulose source and its potential application in food industry – A review. *Heliyon*, 9(14), e18734. http://dx.doi.org/10.1016/j.heliyon.2023.e18734

Zhao, Y., Moser, C., Lindström, M.E., Henriksson, G., & Li, J. (2017). Cellulose nanofibers from softwood, hardwood, and tunicate: preparation–structure–film performance interrelation. *ACS Applied Materials & Interfaces*, *9*(15), 13508-13519. http://dx.doi.org/10.1021/acsami.7b01738